ATMOSPHERIC SCIENCE LETTERS
Atmos. Sci. Let. **15**: 335–341 (2014)
Published online 30 April 2014 in Wiley Online Library
(wileyonlinelibrary.com) **DOI:** 10.1002/asl2.509

RMetS
Royal Meteorological Society

The modulation of tropical storm activity in the Western North Pacific by the Madden–Julian Oscillation in GEOS-5 AGCM experiments

Dongmin Kim,[1] Myong-In Lee,[1]* Hye-Mi Kim,[2] Siegfried D. Schubert[3] and Jin Ho Yoo[4]

[1]*School of Urban and Environmental Engineering, UNIST, Ulsan, South Korea*
[2]*School of Marine and Atmospheric Sciences, Stony Brook University, Stony Brook, NY, USA*
[3]*NASA Goddard Space Flight Center, GMAO, Greenbelt, MD, USA*
[4]*APEC Climate Center, Busan, South Korea*

*Correspondence to:
Prof. Myong-In Lee, School of Urban and Environmental Engineering, Ulsan National Institute of Science and Technology, UNIST-gil 50, Ulju-gun, Ulsan 689-798, Korea.
E-mail: milee@unist.ac.kr

Received: 7 October 2013
Revised: 24 March 2014
Accepted: 8 April 2014

Abstract

This study examines the influence of the Madden–Julian Oscillation (MJO) on tropical storm (TS) activity in the western North Pacific, using observations and GEOS-5 simulations at 50-km horizontal resolution. While GEOS-5 produces an MJO of faster propagation and weaker amplitude, it nevertheless reproduces the observed modulation of TS activity by the MJO with the highest TS genesis and increased track density in the active phases of MJO. The study suggests that the simulation of the sub-seasonal variability of TS activity could be improved by improving the simulations of the MJO in climate models.

Keywords: **tropical storms; MJO; GEOS-5; AGCM**

1. Introduction

The ability of dynamical models to predict tropical storm (TS) activity has been examined in recent studies by substantially increasing the spatial resolution of global climate models (GCMs) up to a few tens of kilometers. LaRow *et al.* (2008) and Zhao *et al.* (2009), for example, showed that the GCMs produced realistic seasonal and interannual variations in the TS number. Much higher spatial resolution models (10-km and higher) simulate reasonable TS activities in sub-seasonal to seasonal time scale (Satoh *et al.*, 2012) and realistic category five hurricanes (Putman and Suarez, 2011). Previous modeling results suggest that a large portion of TS activity (genesis frequency and track) is modulated by large-scale climate variability in the tropics (e.g. El Niño-Southern Oscillation (ENSO), MJO, tropical easterly waves, off-equatorial Rossby waves, and etc.), so it may be predictable at least one season ahead using high-resolution dynamical ensemble prediction systems (Liebmann *et al.*, 1994; Sobel and Maloney, 2000; Kim *et al.*, 2008, and many others). The accuracy of TS simulations is thereby subject to the ability of models to represent the large-scale climate variability, which aspects still have much room for improvement in current climate models.

Previous studies have examined extensively the relationship between ENSO and TS activity using GCMs (e.g. Vitart and Anderson, 2001; Chen and Lin, 2011), quantifying the important thermodynamical impacts of Sea surface temperature (SST) on the main TS development region and their preferred tracks. On the other hand, although there are many observational studies highlighting the important role of the MJO in modulating TS activity on sub-seasonal time scales (Liebmann *et al.*, 1994; Sobel and Maloney, 2000; Kim *et al.*, 2008; Aiyyer and Molinari, 2008; Camargo *et al.*, 2009), only a handful of modeling studies have examined the relationship between TS activity and MJO, particularly over the western North Pacific (WNP) (e.g. Vitart, 2009; Satoh *et al.*, 2012) and the eastern North Pacific (Jiang *et al.*, 2012). The limited number of modeling studies indicates the difficulties of climate models in reproducing the spatial and temporal variability of the MJO and TS. This reflects various deficiencies of current climate models including insufficient horizontal resolution and uncertainties in the parameterized moist physics. Progress on these issues is presented by Vitart (2009) who examined the changes in TS density and the landfall risk according to the MJO propagation. The large-scale patterns of low-level vorticity and the mid-level relative humidity also propagate eastward in the model hindcasts, suggesting important large-scale regulatory mechanisms for the TS development. The very-high resolution GCM runs of Satoh *et al.* (2012) also showed that the eastward propagating MJO and its associated low-level vorticity tends to initiate the TSs, but with different model sensitivity according to the MJO phase from Vitart (2009). Therefore, the simulated relationship between MJO and TS could be model-dependent, being significantly affected by the simulated amplitude and phase of MJOs.

This study revisits the MJO–TS relationship, using long-term simulations of NASA's Goddard

Earth Observing System version 5 (GEOS-5) model (Rienecker *et al.*, 2011) run at 50 km horizontal resolution. The primary focus of this study is to examine whether the model reproduces the observed MJO–TS relationship, and to what extent the dynamical mechanisms (in particular the large-scale forcing associated with the MJO) inferred from the observations and other model simulations are reproduced in this model.

2. Model experiment and data

The GEOS-5 model was integrated at 50 km horizontal resolution from 15 May to 1 December for 12 years (1998–2009). The initial conditions for the atmosphere and land were chosen arbitrarily from previous model integration. The observed weekly SST (Reynolds *et al.*, 2002) was prescribed during the integration. The detection and tracking algorithm for the TSs is based on Camargo and Zebiak (2002), which uses three thresholds for 10 m wind, relative vorticity at 850 hPa, and vertically-integrated temperature anomaly at the TS center. TSs are identified if the values of all three variables exceed two times the standard deviations obtained over the entire basin. Once detected, a storm must last longer than 2 days and the 850 hPa vorticity must be greater than 2.0×10^{-4} s^{-1}. For comparison, we use the International Best Track Archive for Climate Stewardship (IBTrACS; Knapp *et al.*, 2010). For the observations, the TSs whose maximum wind speed is greater than 35 knots are used for the analysis.

The observed MJO was diagnosed by using NOAA interpolated OLR (Liebmann and Smith, 1996) and the zonal wind at 200 and 850 hPa from the Modern-Era Retrospective analysis for Research and Application (MERRA; Rienecker *et al.*, 2011) to compute a combined empirical orthogonal function (EOF). After first removing the climatological mean seasonal cycle for 12 years, the real-time multivariate MJO (RMM) index was calculated for the composite by MJO phase (Wheeler and Hendon, 2004). Only strong MJO events were selected with a RMM index magnitude larger than 1.5. The same procedures were applied for the model simulations. The selected numbers of strong MJO periods are 917 days (38.6% of total days) and 788 days (33.2% of total days) in the observation and GEOS-5, respectively. The simulated MJO is a free simulation by the model only forced by SST, so that the time for MJO occurrence is not the same as observed.

3. MJO simulation in GEOS-5

The GEOS-5 model simulates generally a realistic pattern of the MJO and its life-cycle (Figure 1), but with deficiencies that are common to many other models (Kim *et al.*, 2009). The EOFs of the observations show that main convective region, as indicated by a negative OLR anomaly over the Maritime Continent (EOF1) with low-level convergence and upper-level divergence, moves eastward toward the WNP (EOF2). The simulated EOF structure is in a good agreement with the observed, although the convective signal (OLR) in the model is rather weak and too broad in longitude. The modeled MJO accounts for a comparable fraction of the tropical variability, explaining 18.1% for EOF1 and 12.1% for EOF2, as compared to the observed which explain 17.4% and 14.2%, respectively.

The OLR composites in observation (Figure 1) exhibit the fundamental features of boreal summer intraseasonal oscillation (Kemball-Cook and Wang, 2001; Lawrence and Webster, 2002), with MJO-like eastward propagation along the equator and northward/northwestward propagation over the WNP region. It shows that the negative OLR anomalies start in the Indian Ocean (phases 1 + 2) and propagates eastward through the Maritime Continent (phases 3 + 4). The convective center moves northeast in the WNP and passes across the Date Line (phases 5 + 6), which is followed by a suppression of convection in the WNP (phase 7 + 8). These features are qualitatively captured well in the model simulation, although the simulated propagation speed is too fast over the WNP, specifically when the MJO passes through the equatorial Maritime Continent during phases 3–6. Nevertheless, the observed feature that the convective signal of the MJO propagating from the Maritime Continent to the WNP region and then moving northward is reasonably captured by the model simulation – a feature that is regarded as an important mechanism for the dynamical triggering of TSs (Liebmann *et al.*, 1994; Maloney and Hartmann, 2000).

4. Impacts of the MJO on TS activity

Focusing on the relationship between MJO and TS, Figure 2 shows the percentage of the TS genesis over WNP (100–180°E, 0–40°N) that occurs in each phase of the MJO. During the entire analysis period, a total of 251 TSs were reported in the observation, of which 73 (29%) were identified as developing in strong MJO events. In the model simulation, 60 storms (out of total 208 storms, 29%) were identified as being associated with the strong MJO events, indicating a level of sensitivity to the MJO that is similar to the observed. When the convective center is located in Indian Ocean (phases 1 + 2), the occurrence of TSs is suppressed both in the observations and GEOS-5. The observed TS genesis is still suppressed in phases 3 + 4, whereas the simulated TS occurrence increases to about 2–4 times larger than observed in the same phases. During the active MJO phases over WNP (phases 5 + 6), the number of TS genesis events in the observation and GEOS-5 reaches a maximum, while GEOS-5 shows a weaker transition from the previous phases than the observed. In the simulations, the active phases (5 + 6) account for about 35% of the total TS genesis events, whereas that number is 50% for the observations. The observation

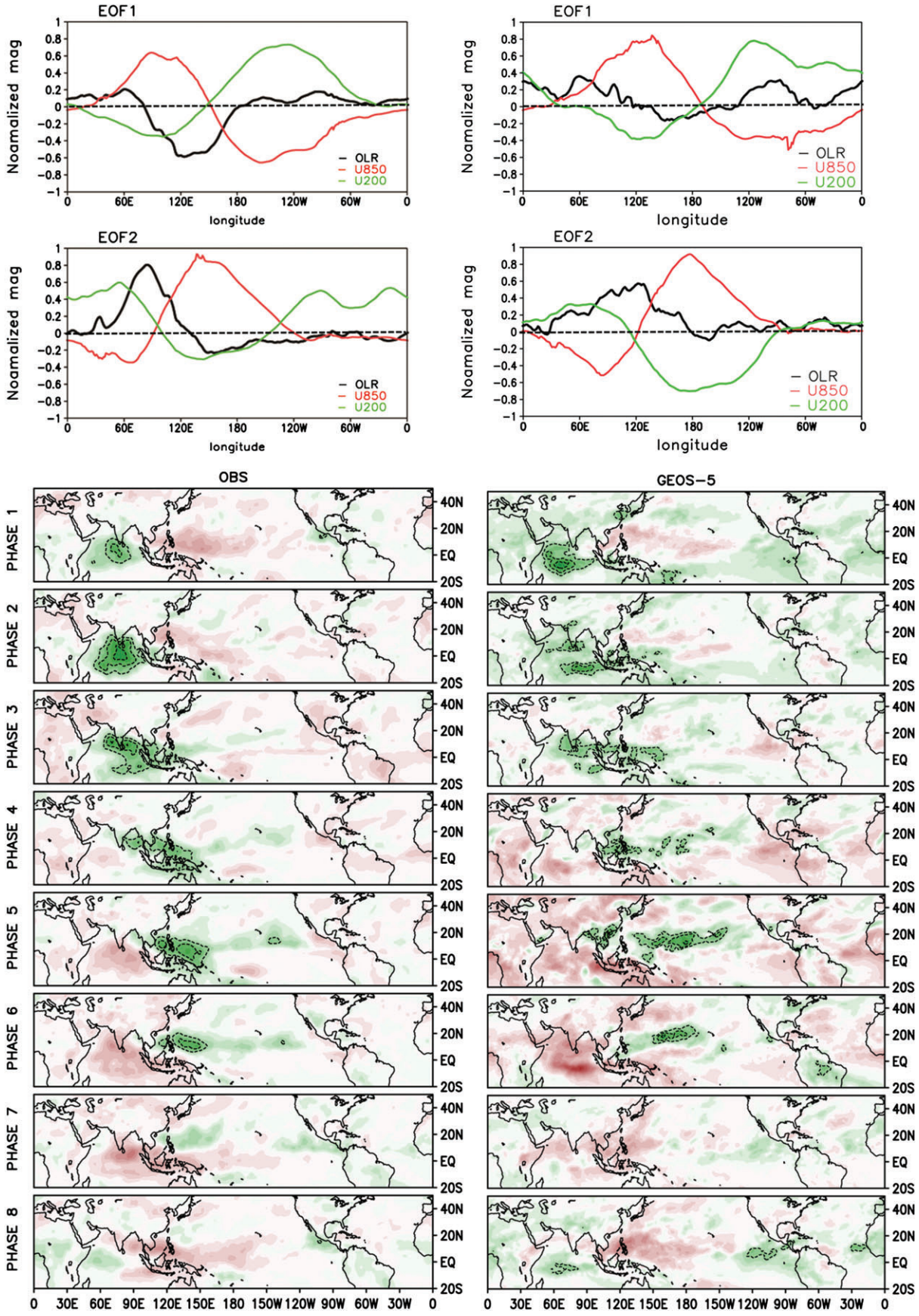

Figure 1. Spatial structure of EOF1 and 2 of the combined EOF analyses of the observation (left) and GEOS-5 (right). Y axis indicates normalized magnitude of three variables in combined EOF analysis. Bottom figures show the OLR anomaly composites according to the phase of MJO from the observation (left) and GEOS-5 (right). Red and blue shading 0 OLR anomalies, where the values less than $-20\,W\,m^{-2}$ are contoured with the $10\,W\,m^{-2}$ interval.

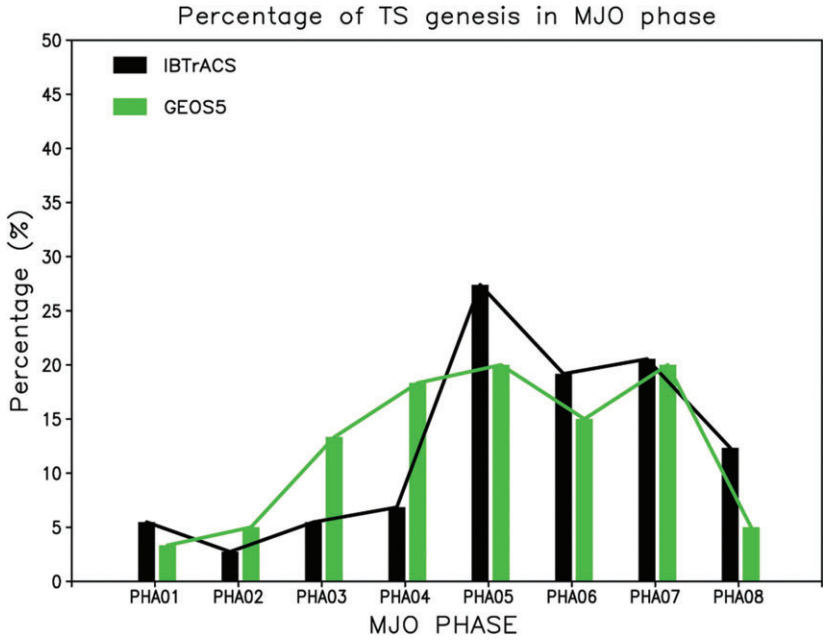

Figure 2. Percentage of tropical storm genesis in the various MJO phases. Black and green bars indicate IBTrACS and GEOS-5, respectively.

and the model simulations both exhibit increase of TS development until the phase 7, and then the number of TSs decreases in the phase 8. Although the simulations show a wider spread of TS genesis events across the MJO phases, the model tends to simulate the maximum development of TSs in phases 5–7, when the MJO activity resides in the main development region (MDR) over the WNP.

The composites of relative vorticity and wind vector anomalies at 850 hPa, and the relative humidity anomalies at 700 hPa over WNP are shown in Figure 3, along with the TS genesis locations. In the observation, westerly (easterly) wind anomalies prevail over the equatorial Western Pacific in the active (suppressed) phase of the TS genesis, which is accompanied by the development of anomalous cyclonic (anticyclonic) vorticity over the MDR in the north. The cyclonic (anticyclonic) vorticity anomalies tend to enhance (suppress) the TS development in the phases 5 + 6 (phases 1 + 2) over the WNP. This interpretation is supported by Maloney and Hartmann (2000), who suggest that anomalously positive (negative) vorticity tends to make favorable (unfavorable) conditions for TS development by increasing (decreasing) meridional wind shear and enhancing (suppressing) dynamical instability (e.g. Schubert *et al.*, 1991). The GEOS-5 AGCM simulations tend to reproduce these observed features reasonably well. Note that TS genesis locations are mostly in the southern flank of the large-scale cyclonic vorticity anomalies over the WNP, suggesting that they are not solely determined by large-scale vorticity. Camargo *et al.* (2009) suggested an important role of the mid-level humidity for the TS development mechanism over the WNP. As shown in Figure 3 for both the observation and the model simulation, the mid-level humidity anomalies, driven by large-scale moisture convergence associated with MJO, provide another favorable condition for TS development. We note that no significant relationship was found between the TS genesis and vertical wind shear anomalies, either in the observations or the model simulation, suggestings that the vertical shear associated with the MJO is not an important factor for TS development over the WNP (Camargo *et al.*, 2009).

Despite the general agreements between the observations and GEOS-5 simulations, significant differences occur in phases 3 + 4, when the convective center propagates across the Maritime Continent. In the observations, the TS development continues to be suppressed as in phases 1 + 2, with a continuation of the low-level easterlies and negative relative vorticity anomalies over the WNP. In contrast, in the model simulations, the westerly wind and positive relative vorticity anomalies appear over the southwestern part of the WNP, which begins to trigger TS development over the South China Sea and Philippines. In case of phases 7 + 8, the observed TS development still exists in the region of anomalous westerlies over the MDR, although the anomalous wind and vorticity forcing decreases with the reduction of TS development. Compared with the observations, the TS development in the model is farther east, following the region of anomalous westerlies and positive vorticity. As a result of the anomalous easterlies and negative vorticity, there is absence of TS development over the western part of the WNP in the simulations. The earlier development and earlier suppression of TSs in the simulations associated with the MJO over the MDR seems to be caused by too fast eastward propagation the MJO. Nevertheless, the basic large-scale dynamical forcing of TS genesis associated with MJO simulated by the GEOS-5 model is qualitatively similar to the observed.

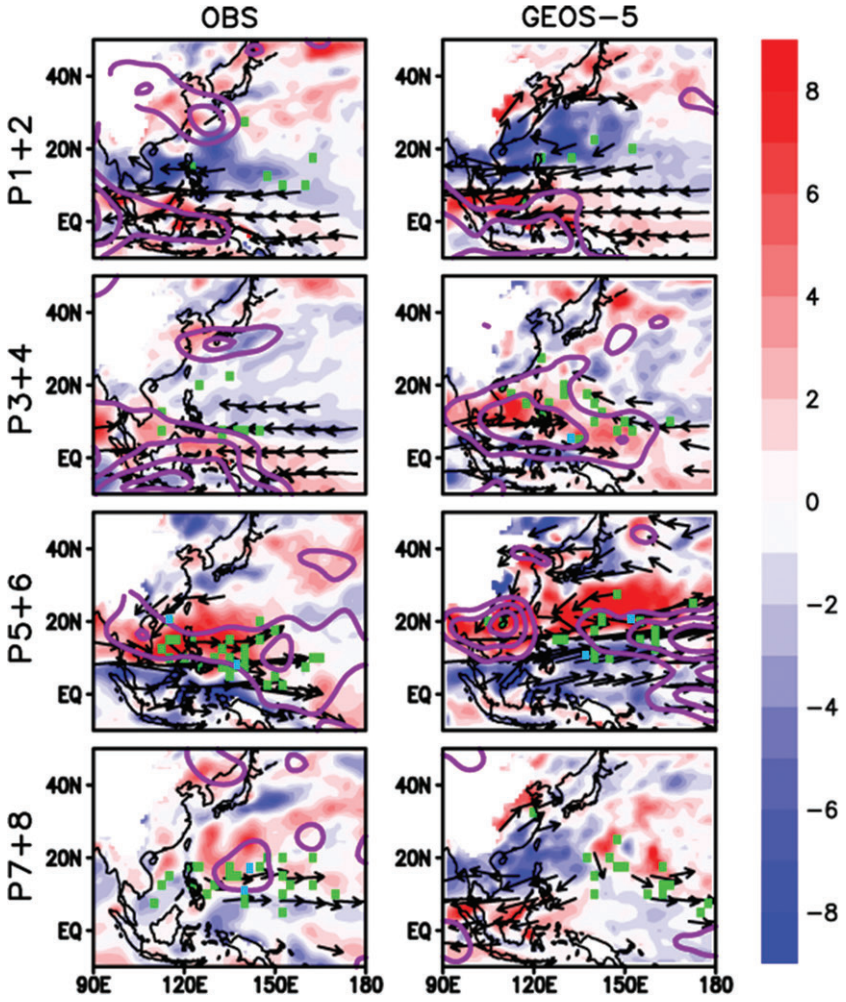

Figure 3. Composites of relative vorticity (multiplied by 10^6, shading, s^{-1}), positive relative humidity at 700 hPa (contoured in 3% interval) and wind vector anomalies (arrow, greater than 2 m s^{-1}) at 850 hPa according to the MJO phases in the observation (left) and the GEOS-5 model simulation (right). The dots in green indicates the location of tropical storm genesis within a 2.5° × 2.5° grid box, and the blue dots indicate the location with more than two storms.

In Figure 4, we examine the time evolution of TS track density anomalies and OLR anomalies with MJO evolution over the WNP region during MJO events. During the inactive phases (1 + 2), both the observations and simulations show negative TS track density anomalies with a positive OLR anomaly in the center of the WNP. After the inactive phases, the convective center propagates from the Indian Ocean to the Maritime Continent (phases 3 + 4) in the observations. Most of the TS track density anomaly in WNP remains negative except for the north part of the Philippines. However, the negative OLR anomalies in GEOS-5 have already migrated into the western part of the WNP because of the faster propagation of the MJO, and as a result, the simulated TS track density anomaly shows positive anomalies in the southwest part of the WNP and negative anomalies in the northeast part of the WNP. During the active phases (5 + 6), the positive TS track density anomalies reside over the WNP both in the observations and the model simulations, which increases the probability of land fall over East Asia. The simulated TS track density anomalies are mostly limited to the south of 30°N. After the active phases (7 + 8), the convective center migrates northeastward, both in the observation and the model simulation. As was the case for the genesis, the model is able to capture the temporal evolution of TS track density associated with the MJO fairly well.

The relationship between the northward propagation of MJO and the TS development is further examined in Figure 5. The GEOS-5 simulation tends to reproduce the signal of northward propagation of convection (as indicated in OLR), and the simulated TS development region is also moving northward following the negative OLR maximum as in the observations. The 850-hPa relative vorticity anomalies are also moving northward (not shown), suggesting a large-scale regulatory mechanism of TS development by MJO.

5. Summary and conclusion

This study has examined the ability of the GEOS-5 AGCM to simulate the impacts of the MJO on the TS activity over the WNP, with a focus on the changes in TS genesis and tracks associated with the different phases

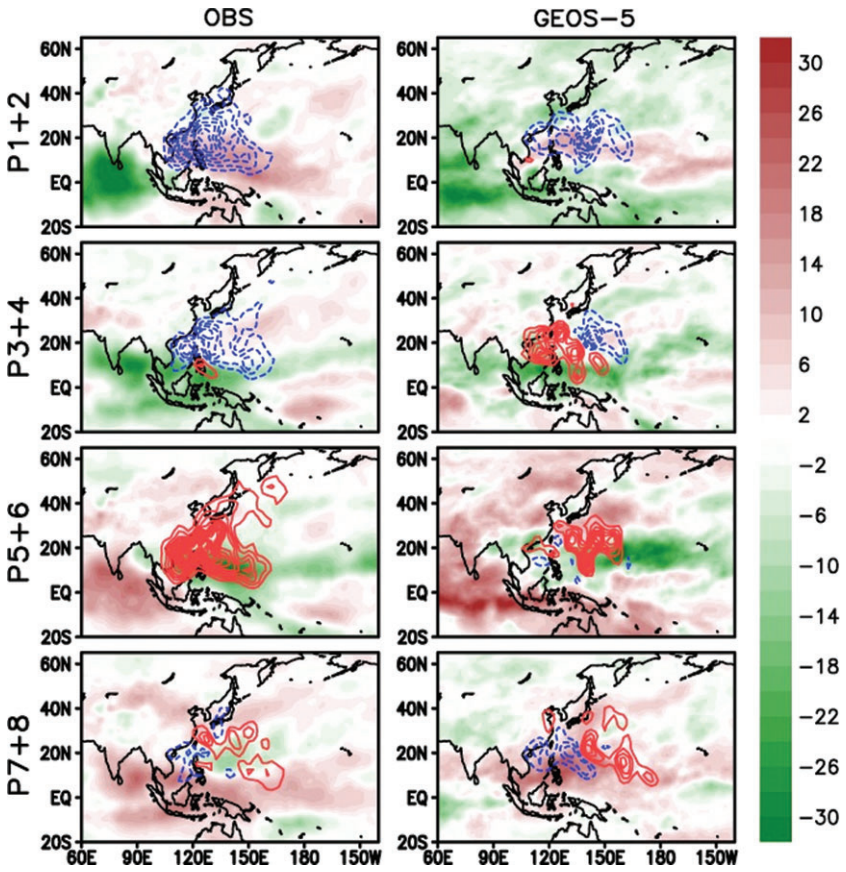

Figure 4. Composites of OLR anomalies (shading in 2 W m^{-2} interval) and the track density anomalies (contoured in 1% interval) according to the MJO phases in the observation (left) and the GEOS-5 simulation (right). Brown and green shading denote the positive and the negative OLR anomalies, respectively. Red and blue contours indicate positive and negative tropical storm track density anomalies, respectively.

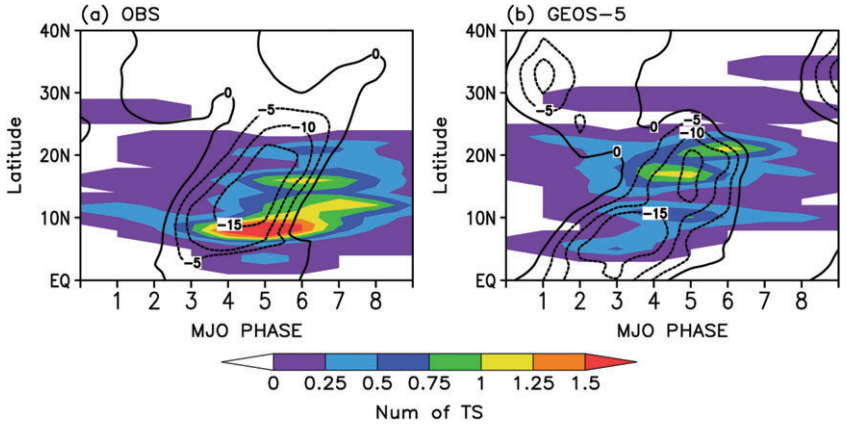

Figure 5. MJO phase-latitude diagram of the TS genesis (shaded) and OLR (black lines, W m^{-2}) anomalies over the TS main development regions (100–160°E). Only negative contours are indicated for OLR. Number of TS genesis was smoothed in space before the phase-latitude composite.

of the MJO. While the simulated MJO propagates too fast to the east with weaker amplitude than the observed, it nevertheless reproduces the basic aspects of the observed sub-seasonal modulation of TS activity associated with the MJO over the WNP region. In particular, the model reproduces the maximum occurrence of TS during the active phases of the MJO, and the minimum occurrence during the suppressed period, as well as the basic dynamical and thermodynamical mechanisms by which the MJO modulates the TS activity. The genesis of TS is enhanced (suppressed) by anomalous westerlies (easterlies), positive (negative) relative vorticity at the low levels and positive (negative) relative humidity at middle levels during the MJO active (inactive) phases. In addition, the TS track changes is also modulated by MJO phases realistically. However, the percentage of the simulated TS genesis events that occur during the active MJO phases over WNP is smaller than

that of the observed, which seems to be related to the model deficiencies in simulating the MJO, that is faster eastward propagation and weaker amplitude compared to the observed MJO (Vitart, 2009; Satoh *et al.*, 2012). These systematic errors are probably related to the earlier peak and the earlier suppression of the TS genesis, the overestimation of TS genesis over the southwest part of the WNP, and the anomalous positive TS track density before the MJO active phases.

The results of this study indicate that the limitations of MJO simulation in climate models is not only a problem for the tropical regions directly influenced by the MJO, but also a problem for simulation and prediction of TS variability in sub-seasonal time scale that have profound societal impacts extending into higher latitudes. This further emphasizes the importance of improving the simulation of the MJO in current climate models.

Acknowledgements

This study was supported by the APEC Climate Center, and the NASA Modeling, Analysis and Prediction (MAP) Program. The authors are grateful for the computing resources provided by NASA and the Supercomputing Center at Korea Institute of Science and Technology Information (KSC-2013-C2-011).

References

Aiyyer A, Molinari J. 2008. MJO and tropical cyclogenesis in the Gulf of Mexico and eastern Pacific: case study and idealized numerical modeling. *Journal of the Atmospheric Sciences* **65**: 2691–2704, DOI: 10.1175/2007JAS2348.1.

Camargo SJ, Zebiak SE. 2002. Improving the detection and tracking of tropical cyclones in atmospheric general circulation models. *Weather and Forecasting* **17**: 1152–1162.

Camargo SJ, Wheeler MC, Sobel AH. 2009. Diagnosis of the MJO modulation of tropical cyclogenesis using and empirical index. *Journal of the Atmospheric Sciences* **66**: 3061–3074, DOI: 10.1175/2009JAS3101.1.

Chen JH, Lin SJ. 2011. The remarkable predictability of inter-annual variability of Atlantic hurricanes during the past decade. *Geophysical Research Letters* **38**: L11804, DOI: 10.1029/2011GL047629.

Jiang X, Zhao M, Waliser DE. 2012. Modulation of tropical cyclones over the eastern Pacific by the intraseasonal variability simulated in an AGCM. *Journal of Climate* **25**: 6524–6538.

Kemball-Cook S, Wang B. 2001. Equatorial waves and air-sea interaction in the boreal summer intraseasonal oscillation. *Journal of Climate* **14**: 2923–2942.

Kim JH, Ho CH, Kim HS. 2008. Systematic variation of summertime tropical cyclone activity in the Western North Pacific in relation to the Madden-Julian Oscillation. *Journal of Climate* **21**: 1171–1191, DOI: 10.1175/2007JCLI1493.1.

Kim D, Sperber K, Stern W, Waliser D, Kang IS, Maloney E, Wang W, Weickmann K, Benedict J, Khairoutdinov M, Lee MI, Neale R, Suarez M, Thayer-Calder K, Zhang G. 2009. Application of MJO simulation diagnostics to climate models. *Journal of Climate* **22**: 6413–6436, DOI: 10.1175/2009JCLI3063.1.

Knapp KR, Kruk MC, Levinson DH, Diamond HJ, Neumann CJ. 2010. The International Best Track Archive for Climate Stewardship (IBTrACS). *Bulletin of the American Meteorological Society* **91**: 363–376, DOI: 10.1175/2009BAMS2755.1.

LaRow TE, Lim YK, Shin DW, Chassignet EP, Cocke S. 2008. Atlantic basin seasonal hurricane simulation. *Journal of Climate* **21**: 3191–3206, DOI: 10.1175/2007JCLI2036.1.

Lawrence DM, Webster PJ. 2002. The boreal summer intraseasonal oscillation: relationship between northward and eastward movement of convection. *Journal of the Atmospheric Sciences* **59**: 1593–1606.

Liebmann B, Smith CA. 1996. Description of a complete (interpolated) outgoing longwave radiation dataset. *Bulletin of the American Meteorological Society* **77**: 1275–1277.

Liebmann B, Hendon HH, Glick JD. 1994. The relationship between tropical cyclones of the Western Pacific and Indian Oceans and the Madden-Julian Oscillation. *Journal of the Meteorological Society of Japan* **72**: 401–411.

Maloney ED, Hartmann DL. 2000. Modulation of eastern North Pacific hurricanes by the Madden-Julian Oscillation. *Journal of Climate* **13**: 1451–1460, DOI: 10.1175/1520-0442(2000)013<1451:MOENPH>2.0.CO;2.

Putman WM, Suarez M. 2011. Cloud-system resolving simulations with the NASA Goddard Earth Observing System global atmospheric model (GEOS-5). *Geophysical Research Letters* **38**: L16809, DOI: 10.1029/2011GL048438.

Reynolds RW, Rayner NA, Smith TM, Stokes DC, Wang W. 2002. An improved in situ and satellite SST analysis for climate. *Journal of Climate* **15**: 1609–1625.

Rienecker MM, Suarez M, Gelaro R, Todling R, Bacmeister J, Liu E, Bosilovich MG, Schubert SD, Takacs L, Kim GK, Bloom S, Chen J, Collins D, Conaty A, Silva A, Gu W, Joiner J, Koster RD, Lucchesi R, Molod A, Owens T, Pawson S, Pegion P, Redder CR, Reichle R, Robertson FR, Ruddick AG, Sienkiewicz M, Woollen J. 2011. MERRA: NASA's modern-era retrospective analysis for research and applications. *Journal of Climate* **24**: 3624–3648, DOI: 10.1175/JCLI-D-11-00015.1.

Satoh M, Oouchi K, Nasuno T, Taniguchi H, Yamada Y, Tomita H, Kodama C, Kinter J, Achuthavarier D, Managanello J, Cash B, Jung T, Palmer T, Wedi N. 2012. The intra-seasonal oscillation and its control of tropical cyclones simulated by high resolution global atmospheric models. *Climate Dynamics* **39**: 2185–2206, DOI: 10.1007/s00382-011-1235-6.

Schubert WH, Ciesielski PE, Stevens DE, Kuo H. 1991. Potential vorticity modeling of the ITCZ and the Hadley circulation. *Journal of the Atmospheric Science* **48**: 1493–1509.

Sobel AH, Maloney ED. 2000. Effect of ENSO and the MJO on Western North Pacific Tropical Cyclones. *Geophysical Research Letters* **27**: 1739–1742.

Vitart F. 2009. Impact of the Madden Julian Oscillation on tropical storms and risk of landfall in the ECMWF forecast system. *Geophysical Research Letters* **36**: L15802, DOI: 10.1029/2009GL039089.

Vitart F, Anderson JL. 2001. Sensitivity of tropical storms frequency to ENSO and interdecadal variability of SST's in a ensemble of GCM integrations. *Journal of Climate* **14**: 533–545, DOI: 10.1175/1520-0442 (2001)014<0.5333:SOATSF>2.0.C.O;2.

Wheeler MC, Hendon HH. 2004. An all-season real-time multivariate MJO index: development of an index for monitoring and prediction. *Monthly Weather Review* **132**: 1917–1932, DOI: 10.1175/1520-0493(2004)132<1917:AARMMI>2.0.CO:2.

Zhao M, Held IM, Lin SJ, Vecchi GA. 2009. Simulations of global hurricane climatology, interannual variability, and response to global warming using a 50-km resolution GCM. *Journal of Climate* **22**: 6653–6678, DOI: 10.1175/2009JCLI3049.1.

